

A two-dimensional hyperbolic spring model for mat foundation in clays subjected to vertical load

Der-Wen Chang^{1a}, Tzu-Min Chou^{1b}, Shih-Hao Cheng^{*2} and Louis Ge^{3c}

¹Department of Civil Engineering, Tamkang University, #151 Ying-Chuan Road, Tamsui District, New Taipei City 251301, Taiwan

²Taiwan Building Technology Center, National Taiwan University of Science and Technology, #43, Sec. 4, Keelung Rd., Taipei City 106335, Taiwan

³Department of Civil Engineering, National Taiwan University, # No. 1, Sec. 4, Roosevelt Rd., Taipei City 106216, Taiwan

(Received October 18, 2023, Revised April 29, 2024, Accepted May 21, 2024)

Abstract. This study proposes a two-dimensional hyperbolic soil spring model for mat foundations in clays subjected to vertically uniform loads to simplify the complexity of three-dimensional finite element analysis on mat foundations. The solutions from three-dimensional finite element analysis were examined to determine the hyperbolic model parameters of the soil springs underneath the slab. Utilizing these model parameters, normalized functions across the middle section of the mat were obtained. The solutions from the proposed model, along with the approximate finite difference analysis of the mat in clays under vertical load, were found to be consistent with those from the three-dimensional finite element analysis. The authors conclude that the proposed method can serve as an alternative for the preliminary design of mat foundations.

Keywords: clay soil; hyperbolic function; mat foundation; nonlinear soil spring; vertically uniform load

1. Introduction

The serviceability performance of the foundation has become increasingly crucial in current foundation design. Structural deformation analysis is essential to predict the load-displacement relationship of the foundation. Two-dimensional (2D) or three-dimensional (3D) finite element (FE) analysis can provide a more robust solution for simulating the nonlinear responses of mat foundations under vertical loads. On the other hand, approximate calculations have also been suggested using a simplified soil spring model. The former requires deployment of constitutive models of soils, while the latter only needs a few model parameters in its applications. Due to the convenience of these calculations, simplified soil spring models have gained popularity in foundation design practice.

The simplified soil spring model of a circular foundation under vertical load can be represented by Lysmer's analog model (Lysmer and Richart 1966). The spring constant (K) for this model is suggested as $4Gr/(1-\nu)$, where G is the shear modulus of the soils, r is the radius of the disc

foundation, and ν is the Poisson's ratio of the soil. The K value is typically used as a single soil spring underneath a rigid foundation (units in F/L). It should be noted that Lysmer's model is applicable to a rigid foundation. In the 1970s, Novak and his colleagues conducted a series of studies on vibrations of an embedded footing. Consequently, approximate frequency-independent springs and dashpots for the surrounding soils have been suggested for various vibration modes of the embedded footing (Novak and Beredugo 1972, Beredugo and Novak 1972, Novak and Sachs 1973). Gazetas (1991) summarized the frequency-dependent dynamic impedance functions for shallow foundations. It should be noted that while these soil springs can be used for static loads, they cannot be applied to nonlinear soil-foundation interaction problems as the solutions were derived based on linear elasticity. Moreover, for mat foundations where the foundation rigidity is relatively low, a group of soil springs is used to support the mat. The modulus of the subgrade reaction (k , units in F/L³) of these soil springs is calculated as the modulus of the subgrade reaction divided by mat displacement.

For the nonlinear analysis of mat foundation responses caused by seismic loads and cyclic superstructural loads, the Beam-on-Nonlinear Winkler Foundation (BNWF) model (Harden and Hutchinson 2009, Muhammad *et al.* 2022) and the Contact Interface (CI) model (Gajan and Kutter 2009) can be referenced. Both soil models consider vertical, horizontal, and rocking modes with linear and nonlinear regions to simulate the spring mechanism. More detailed discussions on the applications of these models can be found in Gajan *et al.* (2010). An overview of the soil-shallow foundation models for nonlinear structural analysis has been recently discussed by Leblouba *et al.* (2016) and

*Corresponding author, Assistant Professor

E-mail: shcheng@mail.ntust.edu.tw

^aProfessor

E-mail: dwchang@mail.tku.edu.tw

^bGraduate student

E-mail: howard52022@gmail.com

^cProfessor

E-mail: louisge@ntu.edu.tw

Deviprasad and Dodagoudar (2020). For discrete modeling with a soil-foundation system under static vertical load, many researchers have adopted and modified a two-parameter model by Pasternak (1954) to model the settlement for 2D mat foundations (Long *et al.* 2021). The shear effects caused by the soil adjacent to the foundation are significant for foundation settlements. Lee *et al.* (2015), Worku and Seid (2020), Zhang *et al.* (2021) discussed the applications of the Pasternak Foundation Model (PFM). The parameters of PFM, including the coefficient of subgrade reactions and the constant of shear influences, are known to be affected by soil stiffness, foundation size, and load distributions. Additionally, the discussions of the nonlinear dynamic responses of the soil foundation can be found in Harada *et al.* (2008), Anastasopoulos *et al.* (2012), and Trombetta *et al.* (2014). Recently, an approximate numerical analysis for raft and rippled raft foundations has been proposed by Jeong *et al.* (2024).

The modulus of subgrade reaction of the subsoil varies beneath the foundation due to the flexibility of the mat. Lee *et al.* (2015), Jeong *et al.* (2017), and Poulos (2018) emphasized that the modulus of subgrade reaction can be influenced by the raft dimensions, subsoil's stiffness, and the applied load. Chang *et al.* (2021) suggested a 2D soil spring model using 3D FE analysis. The model was proposed based on the modulus of the subgrade reaction found at the center of the foundation. Lysmer's analog model was adopted to estimate the k value (i.e., $K/\text{contact area of the mat}$). A modification ratio was suggested to calibrate k for the influence of a flexible foundation. The normalized function of the moduli of subgrade reactions across the middle section of the mat was analyzed to simulate the 2D soil springs underneath the mat foundation.

This spring model was modified by Lysmer's analog soil spring model, which can simulate the variations of the soil spring constants beneath the mat foundation. However, it is only adequate if the modulus of the subgrade reaction is independent of the applied load. The nonlinear load-displacement relations of the mat foundation cannot be captured through such modeling. In this paper, we consider the influences of monotonic load and modify the hyperbolic function of the 2D soil spring model proposed by Chang *et al.* (2021).

2. Hyperbolic function used in geomechanics

The hyperbolic function used in geotechnical engineering can be found by Kondner (1963) in modeling the stress and strain behaviors of cohesive soils. Assuming that the load-displacement relations of the foundation can be approximated as exhibiting hardening behavior, for a mat foundation located in soft clays under vertically monotonic load, the hyperbolic function of the modulus of subgrade reactions (q) underneath the mat with foundation displacements (s) can be expressed in Eq. (1), where the k and q_{ult} are two model parameters. The value k is defined as the initial tangent modulus of the curve, and q_{ult} is the ultimate strength revealed in q - s relations. The application of the hyperbolic function to model the plate load test on gravels has been reported by Wrench (1985).

$$q = \frac{s}{(1/k + s/q_{ult})} \quad (1)$$

On the other hand, the well-known hyperbolic soil model is an alternative application for clays derived from the tri-axial tests (Duncan and Chang 1970). The hyperbolic soil model has often been compared with the hardening soil model (Schanz *et al.* 1999) and can serve as the 3D constitutive law for clays in both drained and undrained conditions. Nowadays, the hyperbolic soil model has been implemented in various computer packages, making it accessible to geotechnical engineers. It should be noted that application of the hyperbolic soil model is more complicated rather than using Eq. (1). The parameters of the model need to be determined experimentally. Frequently, engineers need to define the model behaviors clearly under drained and undrained conditions.

The application of the hyperbolic function to simulate soil-foundation behaviors can be found in Chen *et al.* (2002). The values of k and q_{ult} , along with testing data of the soils, have been discussed. This study adopts the hyperbolic function shown in Eq. (1) more extensively. The q and s obtained from 3D FE analysis were analyzed through numerical studies on loaded mat foundations to determine the parameters k and q_{ult} for nonlinear soil springs allocated at the foundation nodes. These parameters vary across the mat and depend on soil stiffness and foundation width. The proposed modeling presented by Chang *et al.* (2023) will be addressed with more complex expressions in this paper. Such a model can be used for 2D analysis of mat foundations located in the clays with a shear wave velocity of 120-180 m/s, assuming a mat width of 16-36 m and thickness of 1-2 m. The model parameters k and q_{ult} can be easily obtained based on interpolation functions and their suggested values at the center of the mat foundation.

3. Analysis and design of mat foundation

The principles of the mat foundation analysis and design can be found in Ulrich (1991), Horvilleur and Patel (1995), Liou and Lai (1996), Bowles (1997), Fellenius (2014) and Poulos (2018). It has been observed that foundation rigidity and the coefficient of subsoil reaction are critical factors in the calculations. The analysis of mat foundations or piled raft foundations can be categorized as analytical analysis, approximate computer-based analysis, and rigorous computer-based analysis (Poulos 2001). Analytical analysis cannot simulate the spatial variations of the structural system. Approximate computer-based analysis can be conducted using either discrete lumped-mass elements or finite difference (FD) expressions of the governing differential equations of the mat foundation. In nearly all cases, subsoil springs are required to connect with the foundation's nodes. The analysis can be performed as a one-dimensional or multi-dimensional analysis. This method is perhaps the most popular for mat foundation analysis. However, simplifying the soil-foundation system may result in some shortcomings in selecting subsoil springs that can be appropriately distributed underneath the mat.

The FE method is the most representative of rigorous analysis. This analysis is based on solving the equations of motion of the entire structural system. It allows for the full consideration of interaction effects between foundation rigidity and subsoils, distributions of subsoil reactions and foundation settlements, and variations in loads. However, the drawback of such an analysis is that the required computation time is significantly longer than the first two methods. Additionally, preparing the FE mesh and calibrating constitutive model parameters are relatively time-consuming. Once the deformation analysis of the foundation is complete, the structural design of the mat foundation can be carried out (Sert and Kilic 2016, Tabsh *et al.* 2020).

4. Numerical models

To construct a soil spring model suitable for mat foundation analysis, considering the distributions of subsoil reactions influenced by the soil stiffness, foundation size, and load magnitude, the solutions of 3D FE numerical analysis are examined. The 3D FE analysis provides a fundamental basis for establishing the proposed modeling. Assuming a significant vertical uniform load applied to a mat located at the ground surface of clays, the subsoil reactions and the settlements of the mat are computed, and their relationships can be modeled using the hyperbolic function. Model parameters of the hyperbolic functions at various foundation nodes are calibrated by comparing the FE solution with the mathematic results. The variations of these model parameters can be interpolated by the normalized function associated with their values at the center of the mat. With 2D expansions of these interpolating functions and their center values, the hyperbolic function model parameters at arbitrary points of the mat can be obtained. The numerical models in this study are addressed as follows.

4.1 Model geometries and subsoil property

A square mat foundation with widths (B) varying at 16 m, 26 m, and 36 m was assumed. The thickness of the mat was kept at 1 m. The soil profile was considered homogeneous and isotropic clays, with corresponding shear wave velocities (V_s) varied at 120, 140, 160, and 180 m/s. The effect of the groundwater table was temporarily excluded, while the average Poisson's ratio (ν_s) of the soil was maintained at 0.4. Ignoring the groundwater table would provide a more conservative estimation of foundation settlements because the buoyancy of the groundwater is neglected in this case.

For deformation analysis, Young's modulus of the soil (E_s) was obtained from the elasticity equation (i.e., $2V_s^2\rho_s(1+\nu_s) = E_s$, where V_s is the shear wave velocity of the soil, and ρ_s is the mass density of the soil). To simulate more realistic foundation behaviors, the soils were modeled using the Mohr-Coulomb model, allowing rational capturing of soil nonlinearities under monotonic loads. Empirical relationships between E_s and the undrained shear

Table 1 Parameters of the numerical model

Foundation dimensions and applied load	FE zone: 200 m×200 m×60 m for mat width (B): 16 m, 26 m
	FE zone: 300 m×300 m×60 m for mat width (B): 36 m
	The thickness of the mat: 1 m
	Maximum load (p): 220 kPa, 310 kPa, 410 kPa, 530 kPa applied in different cases varying with the soil stiffness
Concrete	$\gamma_c = 24 \text{ kN/m}^3$, $E_c = 30 \text{ GPa}$, $\nu_c = 0.15$
	$\gamma_s = 20 \text{ kN/m}^3$; $\nu_s = 0.4$; $V_s = 120 \text{ m/s}$, 140 m/s, 160 m/s, and 180 m/s; $E_s = 82 \text{ MPa}$, 112 MPa, 146 MPa, and 184 MPa; $S_u = 41 \text{ kPa}$, 56 kPa, 73 kPa, and 92 kPa ($E_s/S_u = 2000$ is assumed for different clays)
Soil	
Interface elements	c_a : adhesion between the concrete and the soil; $c_a = 2/3S_u$; δ : friction angle between concrete and soil ($\delta = 0^\circ$); k_n : normal stiffness, $k_n = 10 E_s$; k_t : tangential stiffness, $k_t = 0.1k_n$

strength (S_u), suggested by Hsieh *et al.* (2003) for clays in Taipei, were used to determine the value of the soil stiffness. The Mohr–Coulomb soil model was adopted to represent monotonic loading conditions. The uniform load (p) was applied incrementally until the foundation started to fail. The load was decomposed into a series of load increments at 10 kPa. An iterative procedure was carried out to ensure the system's equilibrium. Table 1 summarizes the material properties and engineering parameters used in this analysis.

4.2 Discrete mesh and boundaries

The 3D FE analysis was performed using the Midas GTX NX package (Midas 2014) in this study. Eight-node solid elements were used to model the concrete structure and soil, and interface elements were implemented between the concrete and soil. The normal (k_n) and tangent (k_t) stiffnesses of the interface elements were set to be $10E_s$ and E_s , respectively. The ultimate adhesion (c_a) of the interface elements was assumed to be $2/3$ the undrained shear strength (S_u) of clay. The stage construction features in the Midas were utilized. The stability of foundation displacements was ensured by implementing FE dimensions as Fig. 1. Essential boundaries, such as rollers, was placed at the lateral sides and bottom of the FE model, resulting in 2D/3D hinges at the interfaces of these boundaries. To ensure computational efficiency, a one-fourth zone FE mesh was analyzed based on symmetry. The required time was proportional to the resulting foundation settlement in most cases. Fig. 2 depicts the 3D FE mesh of the elements used in the analysis.

5. Interpretation of q - s relations from numerical models

5.1 Back-calculated hyperbolic parameters

The 3D FE analysis was initially conducted to obtain the load-displacement relationships of all the numerical cases. The modulus of subgrade reaction (q) received at the elements across the central section of the mat foundation was plotted against the nodal displacements (s) of the foundation. By doing so, the hyperbolic function can be

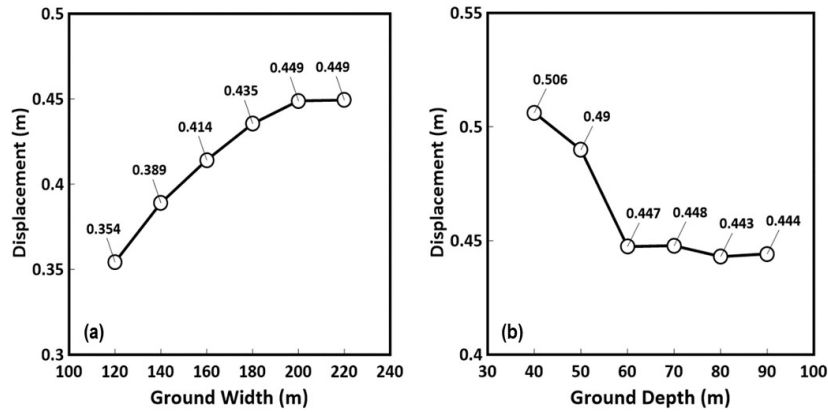


Fig. 1 Stability of the solutions from 3D FE analysis (a) ground width (b) ground depth

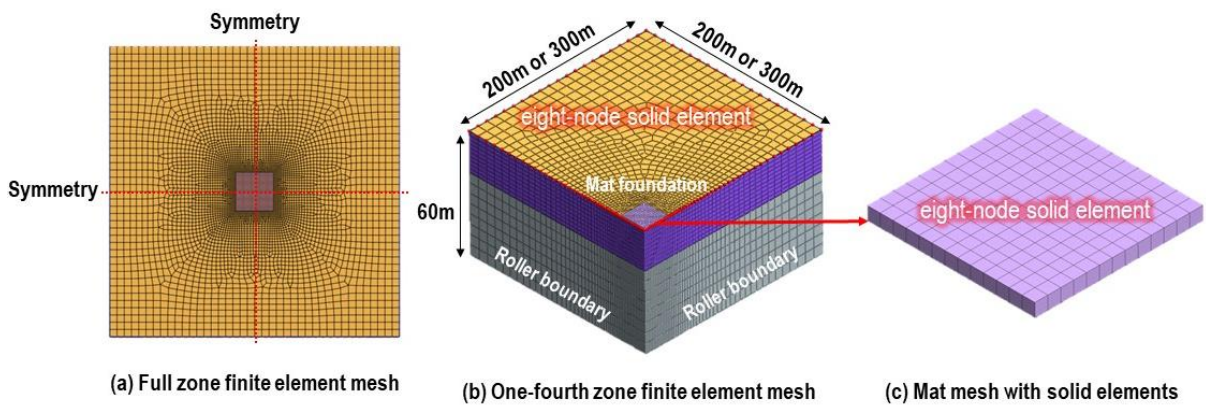


Fig. 2 Layout of 3D FE mesh used in this study

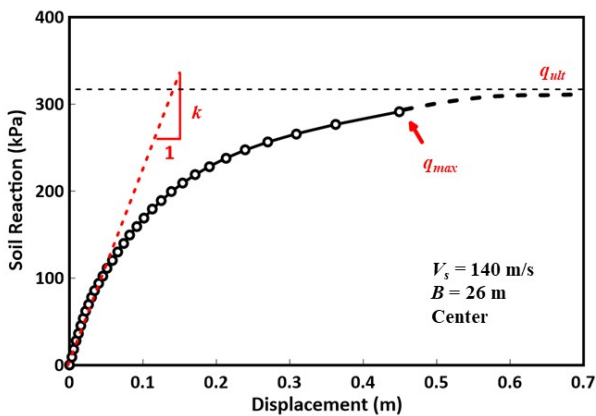


Fig. 3 The relationships of modulus of subgrade reactions and foundation displacements

used to model the curves of q versus s . Taking a square mat foundation with $B = 26$ m and the corresponding $V_s = 140$ m/s as an example, Fig. 3 reveals the modeling where the value of q_{max} denotes the maximum bearing pressure that can be applied before reaching the ultimate load (q_{ult}), representing foundation failure. The ratio of q_{ult}/q_{max} was suggested and evaluated based on the comparisons of the analytical modeling from the equation with the FE results. Therefore, the estimation of q_{ult} can be made. The study suggested ratios of q_{ult}/q_{max} at 1.1-1.4 to yield rational predictions from the hyperbolic functions compared to

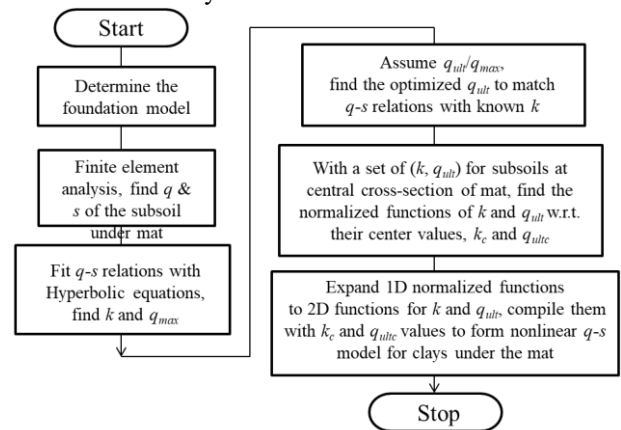


Fig. 4 The flow chart illustrating the simulation procedures of this study

those obtained from FE analysis. Once the appropriate ratio is determined, they can be applied to the further analysis to predict the model parameters, and corresponding simulations proceed as shown in Fig. 4.

Meanwhile, Fig. 5 illustrates the matching results for mats with $B = 26$ m on soils with $V_s = 140$ m/s using q_{max} and q_{ult} , respectively. It can be found that the modification of q_{max} to yield q_{ult} is essential. The values of k and q_{ult} for nodes at the center of the mat foundations studied can be found in the range of 1.2-10.8 MN/m³ (for k) and 264-681 kPa (for q_{ult}). The 3D diagrams showing the variations of k

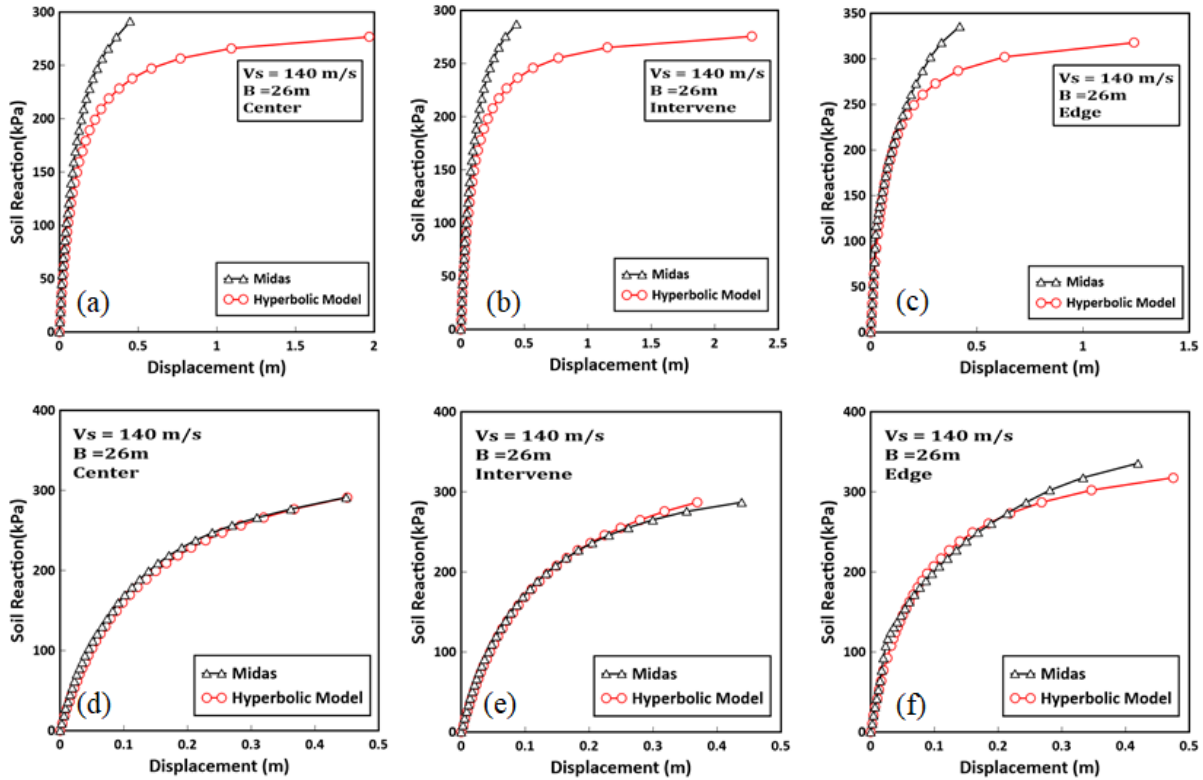


Fig. 5 Hyperbolic modeling of modulus of subgrade reactions and foundation displacements (a), (b) and (c) using q_{max} ; (d), (e), and (f) using q_{ult} .

Table 2 The values of k and q_{ult} obtained in this study

Mat width	Location	Shear wave velocity (m/s)							
		120		140		160		180	
		k (MN/m ³)	q_{ult} (kN/m ²)	k (MN/m ³)	q_{ult} (kN/m ²)	k (MN/m ³)	q_{ult} (kN/m ²)	k (MN/m ³)	q_{ult} (kN/m ²)
16 m	Center	3	213	5	293	7.6	395	10.8	510
	Edge	5	259	7.4	334	10.8	446	14.8	594
	Corner	5	400	9.4	530	13	696	17.6	904
26 m	Center	1.8	203	2.8	291	4.6	405	6.8	524
	Edge	3.4	241	4.8	336	6.8	469	8.8	607
	Corner	4.4	398	6	546	8	719	11.2	909
36 m	Center	1.2	207	1.8	294	2.8	397	4	512
	Edge	2.2	260	3	370	4	473	5.2	629
	Corner	2.8	423	4	578	5.2	748	7.2	953

and q_{ult} for mat foundation with a width of 26 m are presented in Figs. 6 and 7 and are influenced by the subsoil. The corresponding results are also summarized in Table 2.

5.2 Regression analysis

As discussed above, when plotting the values of k and q_{ult} for the hyperbolic soil springs at the nodes across the central section of the foundation, normalized functions of k and q_{ult} can be obtained with respect to their values found at the center of the foundation. Figs. 8-10 depict the variations of the normalized data for k with respect to k_c (at the center) and q_{ult} with respect to q_{ultc} (at the center) for mats of

various widths. Figure 11 depicts the values of k and q_{ult} at the center of the mat. Notice that k_c increases with the soil stiffness and decreases with the mat's width. The value of k_c in the study was found to be in the range of 1.2-10.8 MN/m³. The value of q_{ultc} was found to be approximately the same in the range between 264.4-680.9 kPa, and it is mainly affected by soil stiffness. The normalized functions $f_k(x)$ for k and $f_q(x)$ for q_{ult} have been reported by Chou (2022) using the regression analysis. Table 3 summarizes these normalized functions. Note that they are dependent on the soil stiffness and mat width. As a result, the 2D hyperbolic soil model can be suggested by Eqs. (2) and (3) in association with Eq.(1). In Eqs. (2) and (3), function g is precisely the same as function f , where f is in the x -

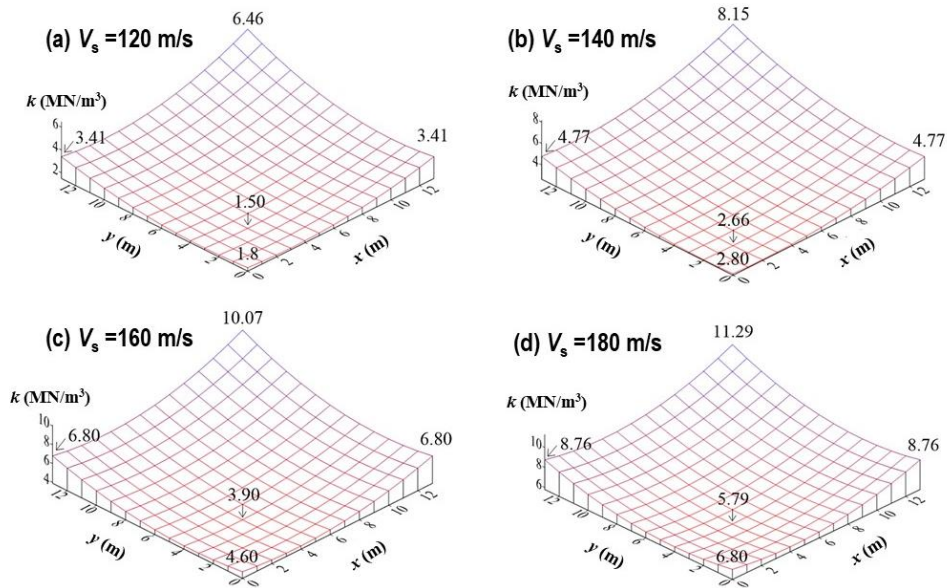


Fig. 6 3D Diagrams of k varied at one-fourth mat foundation at (a) $V_s = 120$ m/s, (b) $V_s = 140$ m/s, (c) $V_s = 160$ m/s and (d) $V_s = 180$ m/s

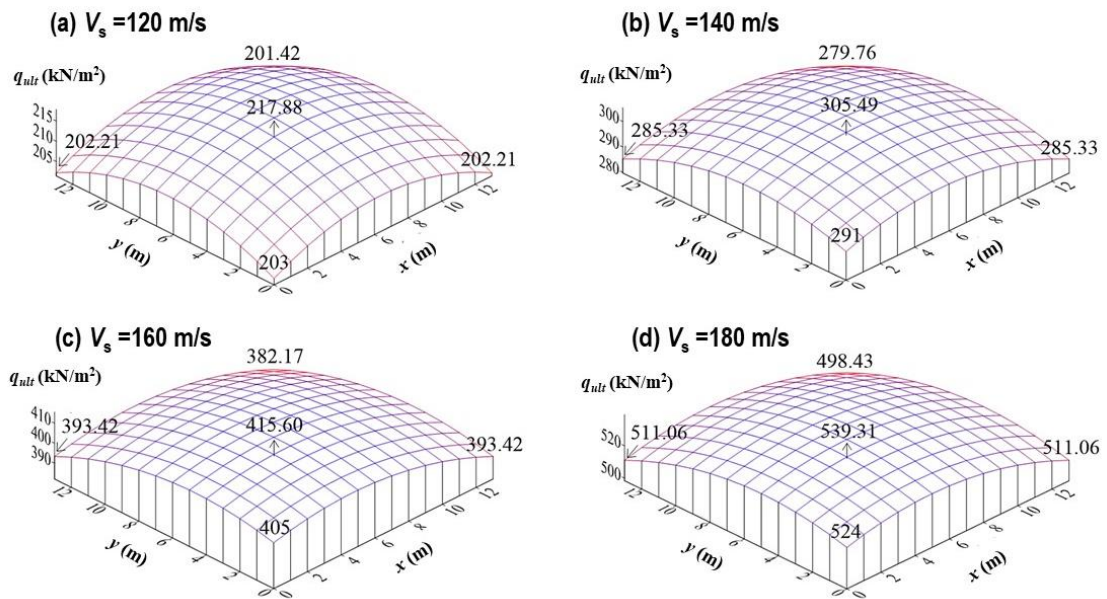


Fig. 7 3D Diagrams of q_{ult} varied at one-fourth mat foundation at (a) $V_s = 120$ m/s, (b) $V_s = 140$ m/s, (c) $V_s = 160$ m/s and (d) $V_s = 180$ m/s

direction, and g is in the y -direction. Function g_k is used for k values, whereas function g_q is used for q_{ult} values. Such modeling can provide the 2D variations of the hyperbolic model parameters k and q_{ult} for the subsoils underneath the mat foundation.

$$k = k_c \times f_k(x) \times g_k(y), \text{ where } f_k(x) = g_k(y) \quad (2)$$

$$q_{ult} = q_{ultc} \times f_g(x) \times g_g(y), \text{ where } f_g(x) = g_g(y) \quad (3)$$

6. Validations of the proposed regression functions

The FD Wave Equation Analysis for Raft Foundation (WERAFT) for the mat foundation using the thin-plate theory was employed to verify the proposed model of the hyperbolic soil springs (Chang *et al.* 2018). The linear soil spring initially implemented in the WERAFT analysis was replaced with the proposed hyperbolic spring model. It is essential to point out that the secant modulus of the subgrade reactions at the mat nodes was computed to form

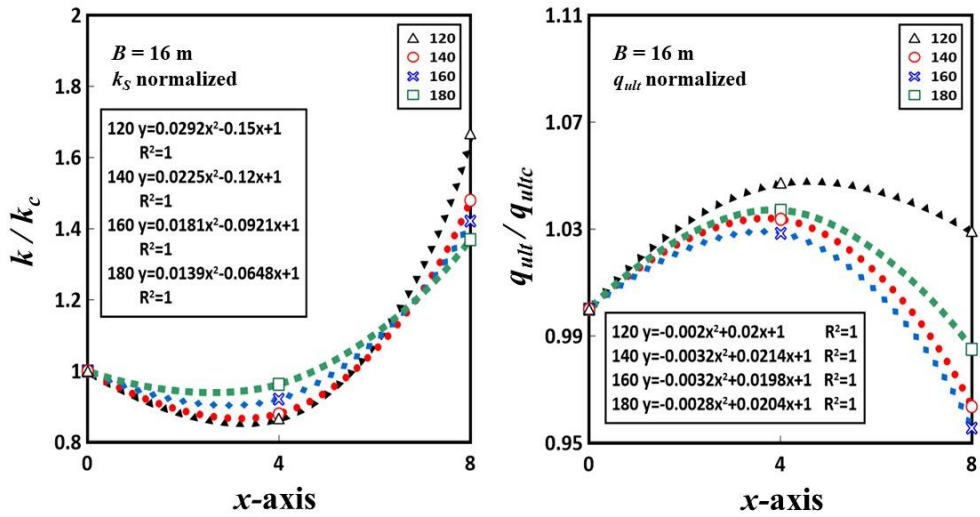


Fig. 8 Variations of the normalized k and q_{ult} for the mat with a width of 16 m

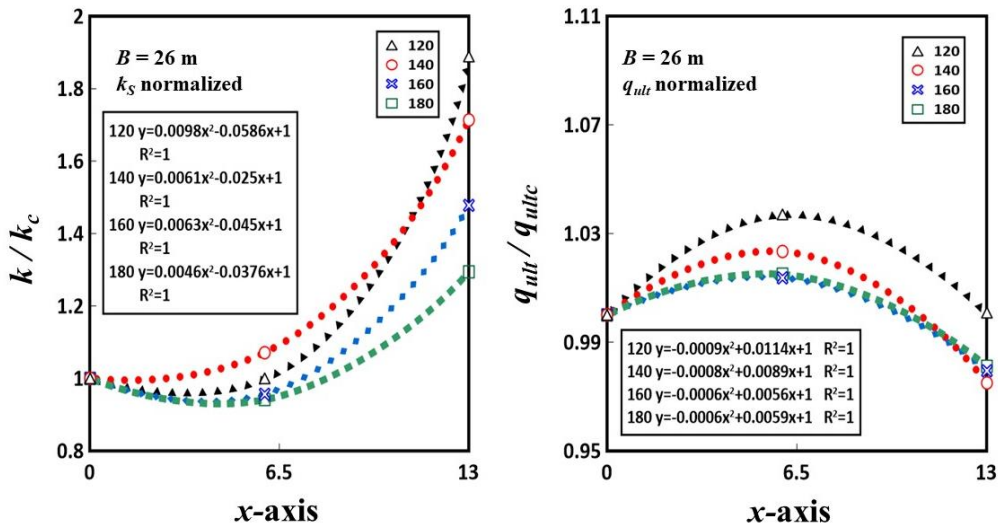


Fig. 9 Variations of the normalized k and q_{ult} for the mat with a width of 26 m

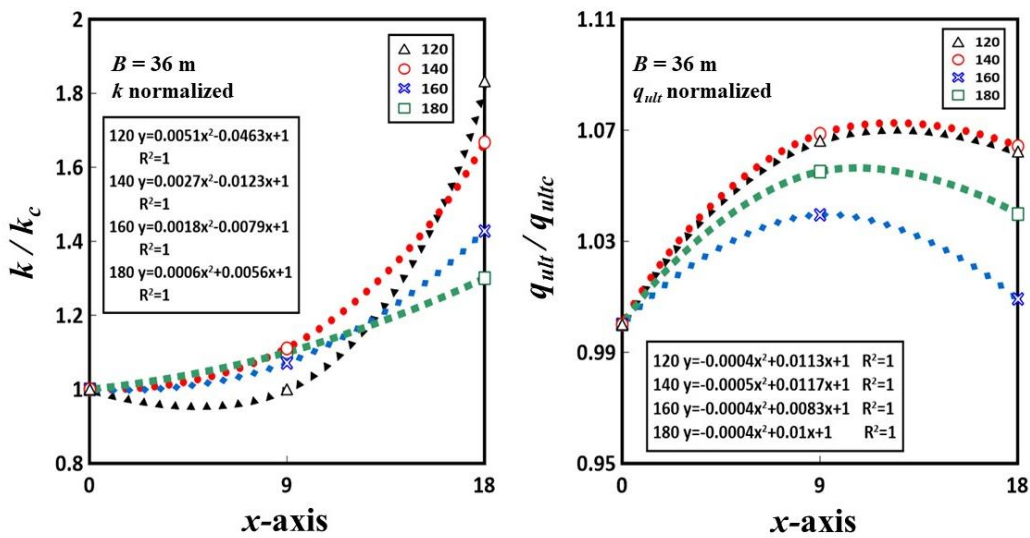


Fig. 10 Variations of the normalized k and q_{ult} for the mat with a width of 36 m

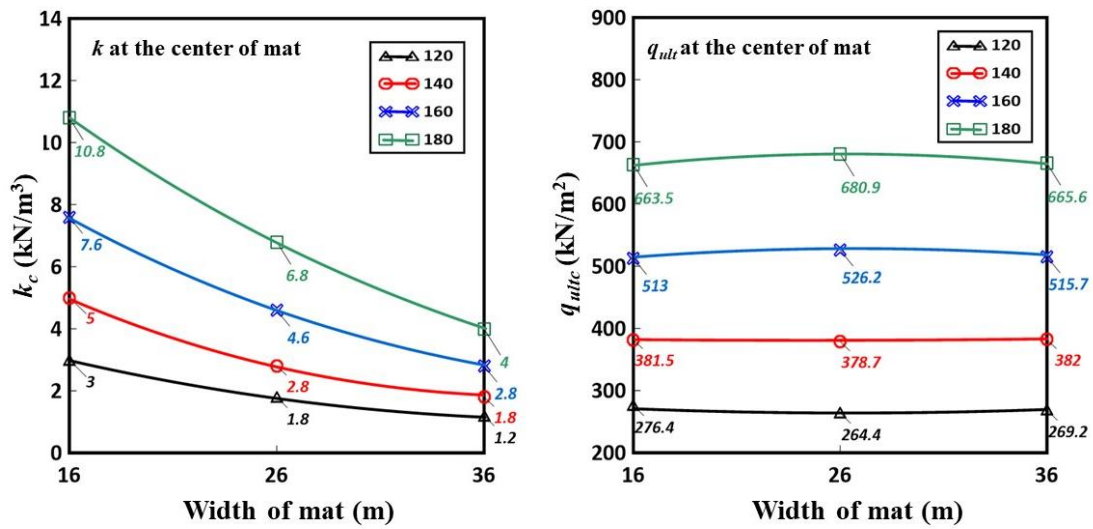


Fig. 11 The values of k and q_{ult} of the soil springs at the center of mat foundations in this study

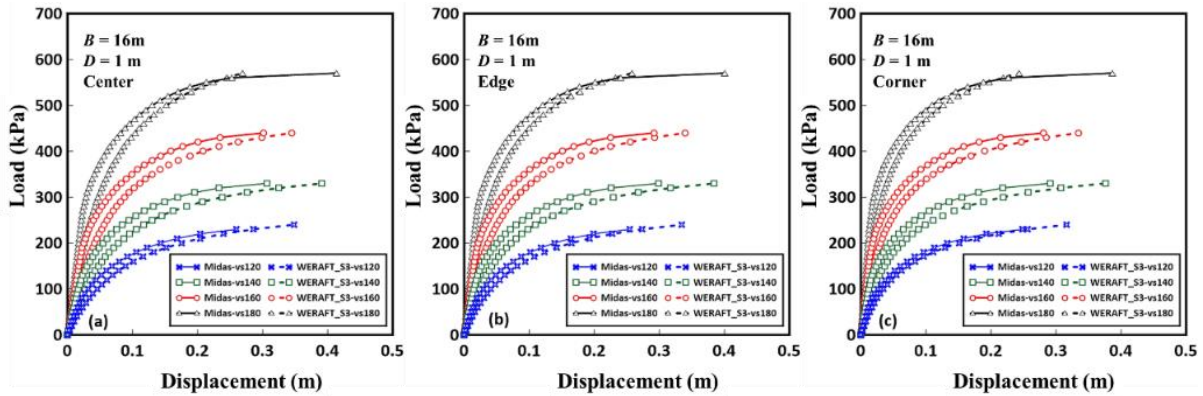


Fig. 12 Comparison of the load-displacement curves from FE and FD analyses in various soils ($B = 16$ m)

Table 3 The normalized functions of f_k for k and f_q for q_{ult} for the soil springs under the mat

V_s (m/s)	Mat Width					
	16 m		26 m		36 m	
	f_q	f_k	f_q	f_k	f_q	f_k
120	$-0.0020x^2+0.0200x+1$	$0.0292x^2-0.1500x+1$	$-0.0009x^2+0.0114x+1$	$0.0098x^2-0.0586x+1$	$-0.0004x^2+0.0113x+1$	$0.0051x^2-0.0463x+1$
140	$-0.0032x^2+0.0214x+1$	$0.0225x^2-0.1200x+1$	$-0.0008x^2+0.0089x+1$	$0.0061x^2-0.0250x+1$	$-0.0005x^2+0.0117x+1$	$0.0027x^2-0.0123x+1$
160	$-0.0032x^2+0.0198x+1$	$0.0181x^2-0.0921x+1$	$-0.0006x^2+0.0056x+1$	$0.0063x^2-0.0450x+1$	$-0.0004x^2+0.0083x+1$	$0.0018x^2-0.0079x+1$
180	$-0.0028x^2+0.0204x+1$	$0.0139x^2-0.0648x+1$	$-0.0006x^2+0.0059x+1$	$0.0046x^2-0.0376x+1$	$-0.0004x^2+0.0100x+1$	$0.0006x^2+0.0056x+1$

the structural stiffness matrix to solve for the foundation displacements. Since the secant modulus of the subgrade reactions depends on the foundation displacements, the equilibriums of the applied load concerning the foundation displacements were ensured using iterative procedures. The solutions from the WERAFT analysis using the 2D hyperbolic soil springs suggested in this study were agreeable with those obtained from 3D FE analysis.

Figs. 12-14 compare the load-displacement curves obtained from the 3D FE analysis with those from the

WERAFT analysis using the proposed soil spring model for the mats on various soils. It can be seen that the proposed model can provide satisfactory predictions on the nonlinear load-displacement relations of the mat with the simplified FD analysis. The mat foundation can be clarified at a width of 16-36 m and a 1-2 m thickness on the said soils where V_s is equal to 120-180 m/s (Chou 2022). The comparison of the largest mat was made for 36 m width. Figs. 15-17 reveal the comparisons of the foundations with various thicknesses. Note that the computational time required for

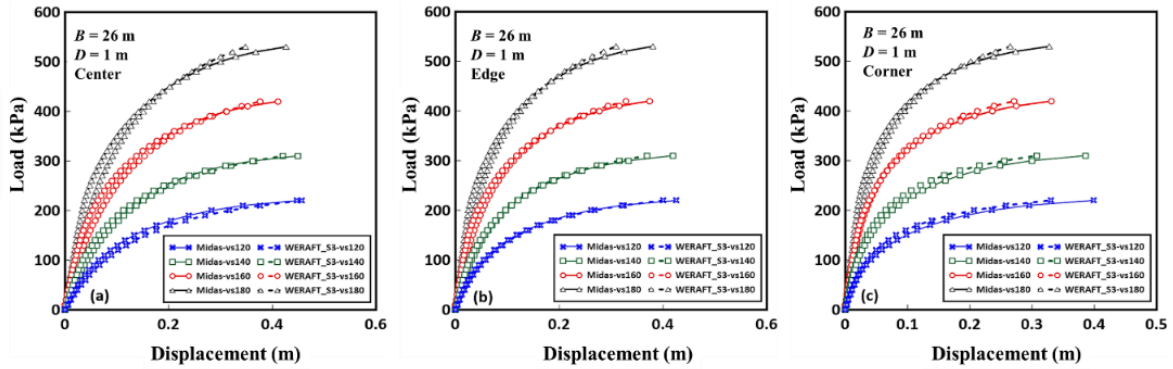


Fig. 13 Comparison of the load-displacement curves from FE and FD analyses in various soils ($B = 26$ m)

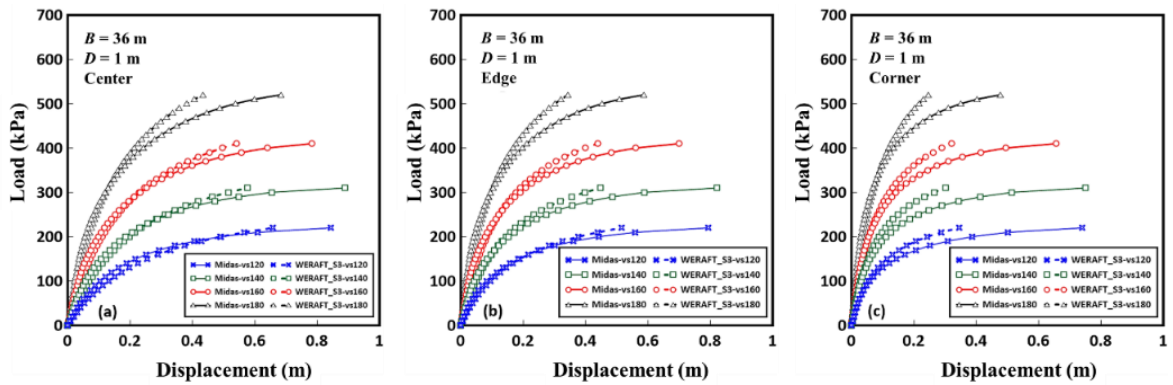


Fig. 14 Comparison of the load-displacement curves from FE and FD analyses in various soils ($B = 36$ m)

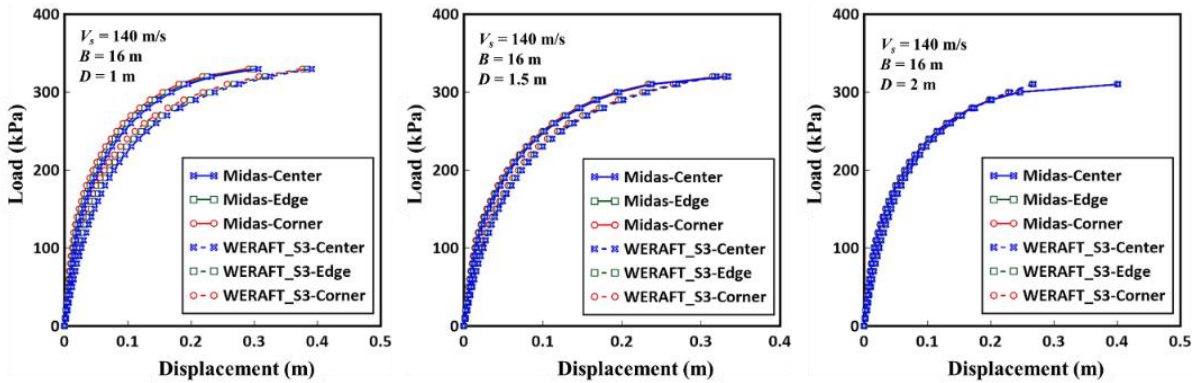


Fig. 15 Comparison of the load-displacement curves from FE and FD analyses varying with the mat thickness ($V_s = 140$ m/s, $B = 16$ m)

Table 4 Comparison of the computation time required of the solutions

Mat width	WERAFT S3	Midas-GTS NX	Time rate
16 m	12 sec	29 min.	1:145
26 m	3 min.	42 min.	1:15
36 m	12 min.	2 hr 18 min.	1:11

the WERAFT analysis is much less than those found in the Midas analysis. Table 4 summarizes the computation time used in 3D FD analysis with the hyperbolic soil springs and those from 3D FE analysis using the Midas GTS NX program. The efficiency of the simplified modeling can be seen clearly.

7. Conclusions

To simplify the complexity of 3D FE analysis on mat foundations, a 2D nonlinear soil spring model is suggested in this study for a vertically loaded mat foundation in clays. The hyperbolic function was adopted to model the nonlinear relationships between the modulus of subgrade reactions and foundation displacements. Model parameters k and q_{ult} were back-analyzed from a 3D FE analysis. The variations of these parameters across the mat were calibrated against the normalized functions. The proposed modeling can be applied to the FD analysis of the mat foundation, yielding comparable results with the 3D FE analysis. The

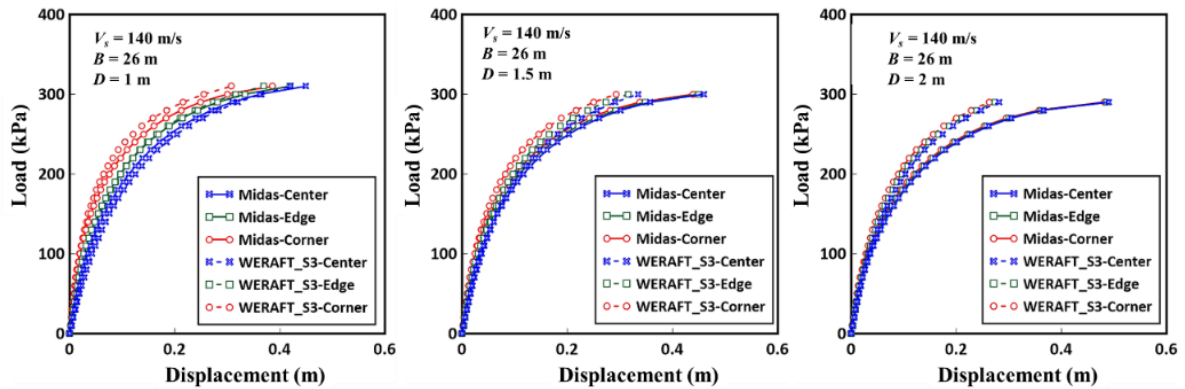


Fig. 16 Comparison of the load-displacement curves from FE and FD analyses varying with the mat thickness ($V_s = 140$ m/s, $B = 26$ m)

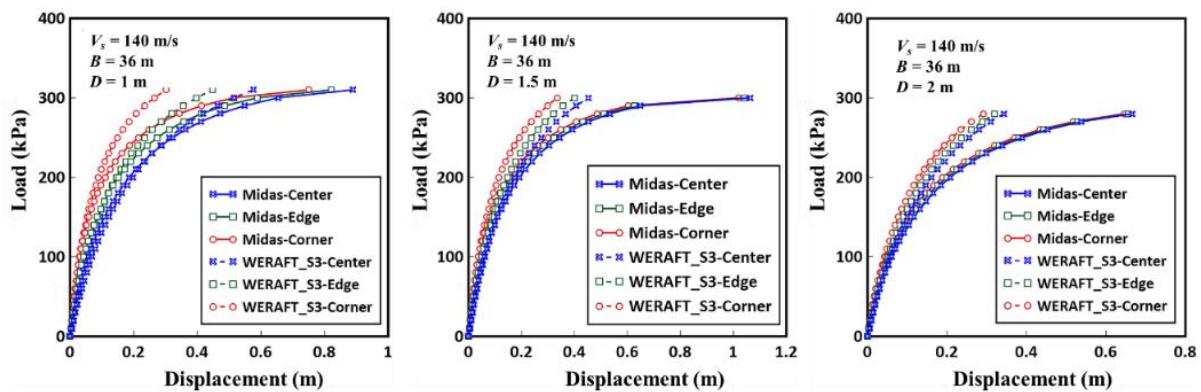


Fig. 17 Comparison of the load-displacement curves from FE and FD analyses varying with the mat thickness ($V_s = 140$ m/s, $B = 36$ m)

corresponding design and model parameters of the proposed model are summarized as follows.

- (1) The proposed 2-D hyperbolic spring model is suitable for flexible mat analysis. The demonstrated mat with widths of 16, 26, and 36 m on top of the homogeneous clay profiles, with the shear wave velocity of the soil varied at 120, 140, 160, and 180 m/s was studied with various vertical loads.
- (2) The ratio between the ultimate bearing pressure (q_{ult}) and the maximum bearing pressure (q_{max}) was found to be around 1.1-1.4. Meanwhile, it was found that soil stiffness is the most influential factor in the mat responses.
- (3) The values of the proposed model parameter (k) at the center of the mat were found to be between 1.2-10.8 MN/m³. They increase with the soil stiffness and decrease as the mat becomes larger. The model parameter q_{ult} at the center was found in the range of 264.4-680.9 kPa, and it mainly increased with soil stiffness.
- (4) Second-order polynomials were obtained as the normalized functions of the model parameters k and q_{ult} across the middle section of the mat. They were expanded in the x - and y -direction with the spatial variables (in meters). The model parameters at the center of the mat are used with these normalized functions to suggest the model parameters of the

hyperbolic function model of the soil springs at an arbitrary point of the mat.

- (5) The secant modulus of the subgrade reaction was computed by dividing the soil reactions by the soil displacement. The proposed soil springs were found applicable to the mat at a thickness of 1-2 m.
- (6) The applicability of this study is limited to the vertically uniform load applied to the mat foundation in clays. Advanced research can be established to include the influences of the inclined and dynamic load.

Acknowledgments

This paper presents a partial result of the research project sponsored by the Ministry of Science and Technology (MOST) in Taiwan. Sincere gratitude is expressed towards the financial support through research grant MOST109-2221-E-032-010-MY2.

References

- Adeel, M.B., Aaqib, M., Pervaiz, U., Rehman, J.U. and Park, D. (2022), "Numerical response of pile foundations in granular soils subjected to lateral load", *Geomech. Eng.*, **28**(1), 11-23. <https://doi.org/10.12989/gae.2021.28.1.011>.

- Anastasopoulos, I., Loli, M., Gelagoti, F., Kourkoulis, R. and Gazetas, G. (2012), "Nonlinear soil-foundation interaction: numerical analysis", *Proceedings of the 2nd Int. Conf. on Performance-Based Design in Earthquake Geotechnical Engineering*, May 28-30, Taormina, Italy.
- Beredugo, Y.O. and Novak, M. (1972), "Coupled horizontal and rocking vibration of embedded footings", *Can. Geotech. J.*, **9**(4), 477-497. <https://doi.org/10.1139/t72-046>.
- Bowles, J.E. (1997), *Foundation Analysis and Design*; McGraw-Hill Pub, 1175.
- Chang, D.W., Lien, H.W. and Wang, T. (2018), "Finite difference analysis of vertically loaded raft foundation based on the plate theory with boundary concern", *J. GeoEng.*, **13**(3), 135-147.
- Chang, D.W., Hung, M.H. and Jeong, S.S. (2021), "Modified lysmer's analog model for two dimensional mat settlements under vertically uniform load", *Int. J. Geomech. Eng.*, **25**(3), 221-231.
- Chang, D.W. and Chou, T.M. (2023), "Developing a two-dimensional nonlinear vertical spring model for mat foundation in clays using hyperbolic function", *Proceedings of the 17th Asian Regional Conference on Soils Mechanics and Geotechnical Engineering*, Astana, Kazakhstan.
- Chen, Q., Xu, T. and Tominaga, K. (2002), "Analytical method for nonlinear behaviour of soil under vertically loaded circular plate", *J. Asian Architect. Build. Eng.*, **1**(2), 1-7. https://doi.org/10.3130/jaabe.1.2_1.
- Chou, T.M. (2022), "Development of nonlinear vertical springs for mat foundations in clays", Master Thesis, Dept. of Civil Engineering, Tamkang University, Taiwan (in Chinese).
- Duncan, J.M. and Chang, C.M. (1970), "Nonlinear analysis of stress and strain in soils", *J. Soil Mech. Found. Division*, **96**(5), 1629-1653.
- Deviprasad, B.S. and Dodagoudar, G.R. (2020), "Seismic response of bridge pier supported on rocking shallow foundation", *Geomech. Eng.*, **21**(1), 73-84. <https://doi.org/10.12989/gae.2020.21.1.073>.
- Fellenius, B. (2014), *Basics of Foundation Design*; electronic edition.
- Gajan, S. and Kutter, B.L. (2009), "Contact interface model for shallow foundations subjected to combined cyclic loading", *J. Geotech. Geoenviron. Eng.*, **135**(3), 407-419. [https://doi.org/10.1061/\(ASCE\)1090-0241\(2009\)135:3\(407\)](https://doi.org/10.1061/(ASCE)1090-0241(2009)135:3(407)).
- Gajan, S., Raychowdhury, P., Hutchinson T.C., Kutter, B.L. and Stewart, J.P. (2010), "Application and validation of practical tools for nonlinear soil-foundation interaction analysis", *Earthq. Spectra*, **26**(1), 111-129. <https://doi.org/10.1193/1.32632>.
- Gazetas, G. (1991), *Foundation Vibrations*. Foundation Engineering Handbook, 553-593.
- Harada, T., Monaka, T., Wang, H., Magoshi, K. and Iwamura, M. (2008), "A nonlinear dynamic soil foundation interaction model using fiber element method and its application to nonlinear earthquake response analysis of cable stayed bridge", *Proceedings of the 14th World Conference on Earthquake Engineering*, Oct. 12-17, Beijing, China.
- Harden, C.W. and Hutchinson, T.C. (2009), "Beam-on-nonlinear-Winkler-foundation modeling of shallow, rocking-dominated footings", *Earthq. Spectra*, **25**(2), 277-300. <https://doi.org/10.1193/1.3110482>.
- Horvilleur, J.F. and Patel, V.B. (1995), "Mat foundation design a soil-structure interaction problem", *ACI*, **152**, 51-94.
- Hsieh, P.G., Kung, T.C., Ou, C.Y. and Tang, Y.G. (2003), "Deep excavation analysis with consideration of small strain modulus and its degradation behavior of clay", *Proceedings of the 12th Asian Regional Conference on Soil Mechanics and Geotechnical Engineering*, Singapore.
- Jeong, S.S., Park, J.J. and Chang, D.W. (2024), "An approximate numerical analysis of rafts and piled-rafts foundation", *Comput. Geotech.*, **168**, 106108. <https://doi.org/10.1016/j.compgeo.2024.106108>.
- Jeong, S.S., Park, J.J., Hong, M.H. and Lee, J.W. (2017), "Variability of subgrade reaction modulus on flexible mat foundation", *Geomech. Eng.*, **13**(5), 757-774. <https://doi.org/10.12989/gae.2017.13.5.757>.
- Kondner, R.L. (1963), "Hyperbolic stress-strain response: cohesive soils", *J. Soil Mech. Found. Eng.*, **89**(1), 115-143.
- Leblouba, M., Toubat, S.A., Rahman, M.E. and Mugheida, O. (2016), "Practical soil-shallow foundation model for nonlinear structural analysis", *Math. Probl. Eng.*, 4514152. <https://doi.org/10.1155/2016/4514152>.
- Lee, J.W., Jeong, S.S. and Lee, J.K. (2015), "3D analytical method for mat foundations considering coupled soil springs", *Geomech. Eng.*, **8**(6), 845-857. <https://doi.org/10.12989/gae.2015.8.6.845>.
- Liou, G.S. and Lai, S.C. (1996), "Structural analysis model for mat foundations", *J. Struct. Eng.*, **122**(9), 1114-1117. [https://doi.org/10.1061/\(ASCE\)0733-9445\(1996\)122:9\(1114\)](https://doi.org/10.1061/(ASCE)0733-9445(1996)122:9(1114)).
- Long, W.S., Limkatanyu S., Hansapinyo, C., Prachasaree, W., Rungamornrat, J. and Kwon, M. (2021), "Nonlinear flexibility based beam element on Winkler Pasternak foundation", *Geomech. Eng.*, **24**(4), 371-388. <https://doi.org/10.12989/gae.2021.24.4.371>.
- Lysmer, J. and Richart, F.E. (1966), "Dynamic response of footings to vertical loading", *J. Soil Mech. Found. Division*, **92**(1). <https://doi.org/10.1061/JSFEAQ.0000084>.
- Midas (2017), *Midas GTS NX User Manual*, Midas IT Co.
- Novak, M. and Beredugo, Y.O. (1972), "Vertical vibrations of embedded footings", *J. Soil Mech. Found. Division*, **98**(12), 1291-1331. <https://doi.org/10.1061/JSFEAQ.00018>.
- Novak, M. and Sachs, K. (1973), "Torsional and coupled vibrations of embedded footings", *Earthq. Eng. Struct. D.*, **2**(1), 11-33. <https://doi.org/10.1002/eqe.4290020103>.
- Pasternak, P.L. (1954), "On a new method of analysis of an elastic foundation by means of two constants", Gosudarstvennoe Izdatelstvo Literaturi po Stroitelstvu Arkhitekture, Moscow. (In Russian)
- Poulos, H.G. (2018), "Rational assessment of modulus of subgrade reaction", *Geotech. Eng. J. SEAGS and AGSSEA*, **49**(1), 1-7.
- Poulos, H. (2001), "Piled raft foundations: design and applications", *Geotechnique*, **51**(2), 95-113. <https://doi.org/10.1680/geot.2001.51.2.95>.
- Schanz, T., Vermeer, P.A. and Bonnier, P.G. (1999), "The hardening soil model: Formulation and verification", Beyond 2000 in Computational Geotechnics – 10 Years of PLAXIS; Balkema, Rotterdam.
- Sert, S. and Kılıç, A.N. (2016), "Numerical investigation of different superstructure loading type effects in mat foundations", *Int. J. Civil Eng.*, **14**, 171-180. <https://doi.org/10.1007/s40999-016-0013-6>.
- Tabsh, S.W., El-Emam, M. and Partazian, P. (2020), "Numerically based parametric analysis of mat foundations", *Practice Periodical on Structural Design and Construction*, **25**(2), 04020009. [https://doi.org/10.1061/\(ASCE\)SC.1943-5576.000047](https://doi.org/10.1061/(ASCE)SC.1943-5576.000047).
- Trombetta, N.W., Mason, B., Hutchinson, T., Zupan, J.D., Bray, J., and Cutter, B.L. (2014), "Nonlinear soil-foundation-structure and structure-soil-structure interaction: centrifuge test observations", *J. Geotech. Geoenviron. Eng. ASCE*, **140**(5), 04013057. [https://doi.org/10.1061/\(ASCE\)GT.1943-5606.0001074](https://doi.org/10.1061/(ASCE)GT.1943-5606.0001074).
- Ulrich, E. (1991), "Subgrade reaction in mat foundation design", *Concrete Int.*, **13**(4), 41-50.
- Worku, A. and Seid, T. (2020), "Application of a robust subgrade model in the analysis of plates on an elastic foundation", *Int. J. Geomech.*, **20**(10), 0001834.

[https://doi.org/10.1061/\(ASCE\)GM.1943-5622.0001834](https://doi.org/10.1061/(ASCE)GM.1943-5622.0001834).

Wrench, B.P. (1985), "Plate tests for the measurement of modulus and bearing capacity of gravels", *Civil Eng. Siviele Ingenieurswese*, **10**, 547.

Zhang, W.X., Lv, W.L., Zhang, J.Y., Wang, X., Hwang, H.J. and Yi, W.J. (2021), "Energy-based dynamic parameter identification for Pasternak foundation model", *Earthq. Eng. Eng. Vib.*, **20**, 631-643. <https://doi.org/10.1007/s11803-021-2043-6>.

JS